JACS
JOURNAL OF THE AMERICAN CHEMICAL SOCIETY
Article
pubs.acs.org/JACS

Spectroscopic Investigations of Catalase Compound II: Characterization of an Iron(IV) Hydroxide Intermediate in a Non-thiolate-Ligated Heme Enzyme

Timothy H. Yosca,[†] Matthew C. Langston,[‡] Courtney M. Krest,[§] Elizabeth L. Onderko,[‡] Tyler L. Grove,[‡] Jovan Livada,[‡] and Michael T. Green*[,†]

[†]Departments of Chemistry & Molecular Biology and Biochemistry, University of California, Irvine, California 92697, United States
[‡]Department of Chemistry, Pennsylvania State University, University Park, Pennsylvania 16802, United States
[§]Stanford Synchrotron Radiation Lightsource, SLAC National Accelerator Laboratory, Menlo Park, California 94025, United States

Supporting Information

ABSTRACT: We report on the protonation state of *Helicobacter pylori* catalase compound II. UV/visible, Mössbauer, and X-ray absorption spectroscopies have been used to examine the intermediate from pH 5 to 14. We have determined that HPC-II exists in an iron(IV) hydroxide state up to pH 11. Above this pH, the iron(IV) hydroxide complex transitions to a new species (pK_a = 13.1) with Mössbauer parameters that are indicative of an iron(IV)-oxo intermediate. Recently, we discussed a role for an elevated compound II pK_a in diminishing the compound I reduction potential. This has the effect of shifting the thermodynamic landscape toward the two-electron chemistry that is critical for catalase function. In catalase, a diminished potential would increase the selectivity for peroxide disproportionation over off-pathway one-electron chemistry, reducing the buildup of the inactive compound II state and reducing the need for energetically expensive electron donor molecules.

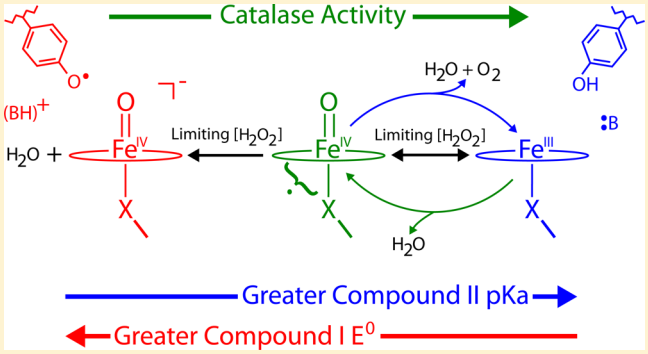

INTRODUCTION

Iron(IV)-oxo complexes play critical roles in biology. The ferryl moiety is found at the core of reactive intermediates in peroxidases, oxidases, monooxygenases, and halogenases.[1−9] These oxidizing complexes were first observed in heme proteins in the 1940s,[10] but they were not fully characterized until the second half of the last century.[11−17] With the characterization of these intermediates came a flurry of synthetic work aimed at modeling these species.[18−20] The interplay between these two lines of investigations led to considerable insight into the structure (both electronic and geometric) as well as the function of these high-valent systems.[13−17,20−23] As a result of these efforts, it is now well understood that in heme proteins the ferryl moiety lies at the center of two reactive intermediates called compound I and compound II.[2] Prototypical compound I species are best described as ferryl porphyrin radicals,[24−27] while prototypical compound II species are the iron(IV)-oxo porphyrins obtained by the one electron reduction of compound I.[28]

More recently, a new type of compound II complex was identified: the iron(IV) hydroxide (or protonated ferryl) complex.[29−34] These unusual intermediates have been characterized in several thiolate-ligated heme proteins. Cytochrome P450, chloroperoxidase (CPO), and aromatic peroxygenase (APO) have all been prepared in the Fe(IV)OH state. Importantly, these are the only heme enzymes that are known to activate C−H bonds, and the elevated pK_a of these systems has been suggested to play an important role in facilitating C−H bond cleavage.[34]

It has been argued that basic ferryls can govern the partition between one- and two-electron chemistry.[34,35] P450s with a strongly donating thiolate ligand (and an elevated iron(IV) hydroxide pK_a) primarily function through two-electron oxidations, while histidine-ligated peroxidases typically operate through sequential one-electron events. Simple arguments based on Marcus theory suggest that the elevated compound II pK_a in P450 suppresses the rate constant for one-electron oxidations of the protein superstructure by a factor of 10 000 relative to histidine-ligated systems, promoting C−H bond cleavage and subsequent substrate hydroxylation in the process.[34]

In efforts to explore the connection between the iron(IV) hydroxide pK_a and reactivity, researchers have sought to prepare iron(IV) hydroxide species in synthetic model compounds and other heme proteins. To date, a definitive characterization of a synthetic iron(IV) hydroxide remains elusive, and only authentic iron(IV)-oxos have been observed

Received: September 15, 2016
Published: November 9, 2016

ACS Publications © 2016 American Chemical Society

DOI: 10.1021/jacs.6b09693
J. Am. Chem. Soc. 2016, 138, 16016−16023

in histidine-ligated peroxidases and globins.[12,28,36−44] Although it is thought that hydrogen-bonding interactions in peroxidases imbue the axial histidine ligand with imidazolate character (believed to be important for activating the O−O bond of hydrogen peroxide and stabilizing the high-valent oxo intermediates),[3,15,22] the degree of electron donation generated by this mechanism appears to be insufficient to stabilize the iron(IV) hydroxide state ($pK_a \leq 3.5$).[28,34,35]

One enzymatic system that remains of interest with respect to the existence and characterization of an iron(IV) hydroxide intermediate is the heme enzyme catalase. Catalase utilizes two-electron chemistry to disproportionate hydrogen peroxide into oxygen and water.[1] The enzyme possesses an axial tyrosinate ligand, the anionic charge of which is similar to that of the thiolate. Additionally, a tyrosinate ligand has been found to be donating enough to stabilize an iron(IV) intermediate in the Tyr-Fe(IV)-His-ligated heme of the enzyme MauG.[45] As a result, one might expect this ligation to produce a basic ferryl species, but heme catalases also possess a highly conserved arginine residue that hydrogen bonds to the oxygen atom of the tyrosinate ligand in a "bidentate" fashion, Figure 1.[1,46,47] Do non-covalent interactions with the cationic arginine residue reduce the effective tyrosinate charge seen by the ferryl moiety?

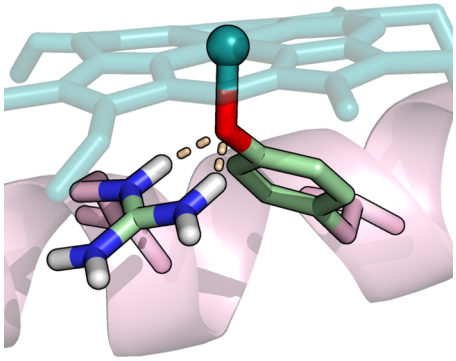

Figure 1. Active site of catalase from the crystal structure of HPC (PDB ID: 2A9E). A conserved arginine residue hydrogen bonds to the oxygen atom of the tyrosinate ligand in a "bidentate" fashion.

The available data for catalase compound II are inconsistent. Resonance Raman experiments have indicated an authentic ferryl species,[48] while X-ray crystallographic studies have reported an iron(IV) hydroxide center.[46b,47] Given the tendency of high-valent centers to be reduced in the X-ray beam, one must be careful when assigning metal oxidation states in crystal structures.[28,35,36] The distance of 1.87 Å reported for the Fe−O bond in ferryl catalase is too long to be associated with an iron(IV) intermediate, suggesting the crystal was reduced in the beam.[47]

Additional experiments used EXAFS and Mössbauer spectroscopies to study ferryl catalase at varying pH.[49,50] The data obtained from these investigations were interpreted in terms of a mixture of protonated and unprotonated ferryl intermediates. However, the samples were not pure, and the ratio of the putative protonated and unprotonated species did not change reversibly with pH, suggesting the intermediates were not simply linked by a protonation event.

Given the interest in iron(IV) hydroxide species and their use in promoting two-electron chemistry, we sought to clarify the nature of ferryl catalase. Here we present UV/visible, Mössbauer, and extended X-ray absorption fine structure (EXAFS) data for *Helicobacter pylori* catalase (HPC). Our measurements show that ferryl catalase is protonated over a wide pH range ($pK_a > 11$).

RESULTS AND DISCUSSION

UV/Visible Spectroscopy. During the course of purifying ferric enzyme for the preparation of compound II (HPC-II), we observed that ferric catalase could be obtained in two pH- and [NaCl]-dependent forms, which are visibly distinguished by their respective colors, green or brown. Ferric HPC is green under conditions of low pH and high salt (pH < 5, [NaCl] ≥ 250 mM). With increasing pH, the color of the protein turns brown ($pK_a \approx 6$). Brown enzyme can also be obtained at low pH with low salt (pH < 5, [NaCl] ≤ 100 mM). The UV/visible sprectra of the green and brown forms are shown in Figure 2.

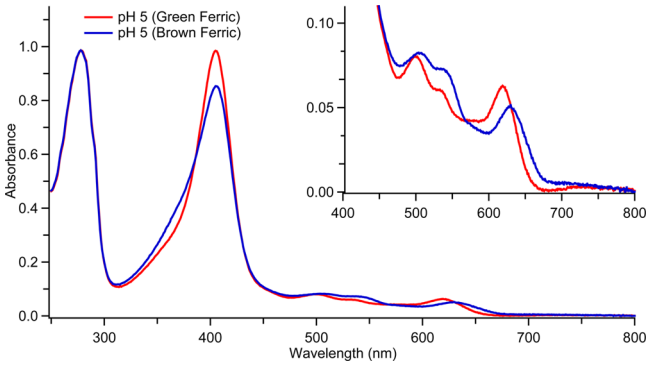

Figure 2. UV/visible spectra of green (500 mM NaCl) and brown (0 mM NaCl) HPC at pH 5 (50 mM citrate buffer). The concentration of HPC is ∼10 μM.

Mössbauer measurements (see below) yield very similar parameters for the green and brown forms of ferric HPC. These parameters are indicative of a high-spin ferric center.[51,52] Importantly, either ferric form can be reacted with peracetic acid to obtain catalase compound II (which is red in color).

The UV/visible spectra of HPC-II obtained from brown and green HPC are shown in Figures 3−5. HPC-II obtained from green HPC has a spectrum with a Soret maximum at 431 nm and an α Q-band intensity that is slightly larger than the β band intensity ($\alpha/\beta \approx 1.1$). HPC-II obtained from brown HPC has a Soret maximum at 429 nm and has a slightly different ratio of

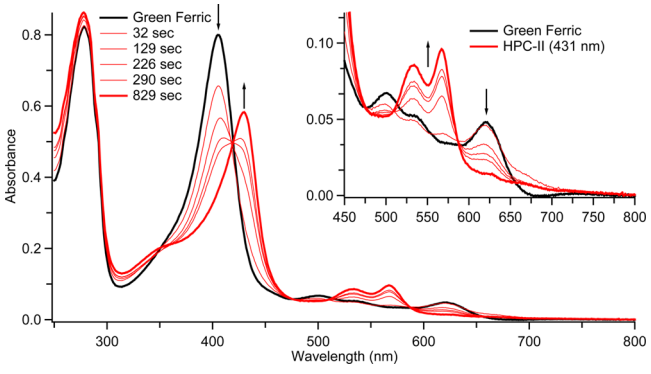

Figure 3. UV/visible spectra of HPC-II at pH 5 (50 mM citrate buffer, 500 mM NaCl) made from the reaction of green HPC and 12.5 equiv of PA. No significant buildup of compound I occurred prior to compound II formation. The Q-band ratio is ∼1.1 (α/β).

DOI: 10.1021/jacs.6b09693
J. Am. Chem. Soc. 2016, 138, 16016−16023

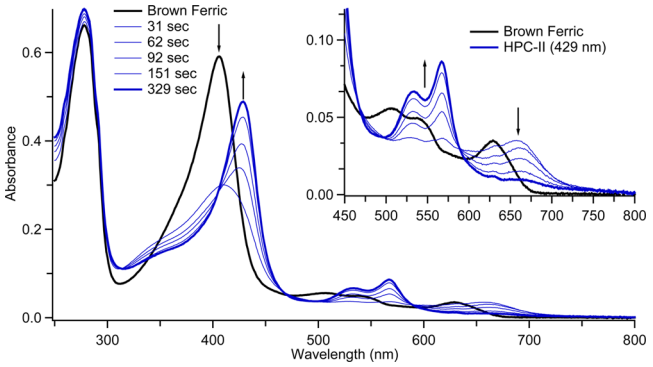

Figure 4. UV/visible spectra of HPC-II at pH 5 (50 mM citrate buffer, 0 mM NaCl) made from the reaction of brown HPC and 12.5 equiv of PA. Significant buildup of compound I occurs prior to compound II formation. The Q-band ratio is ~1.3 (α/β).

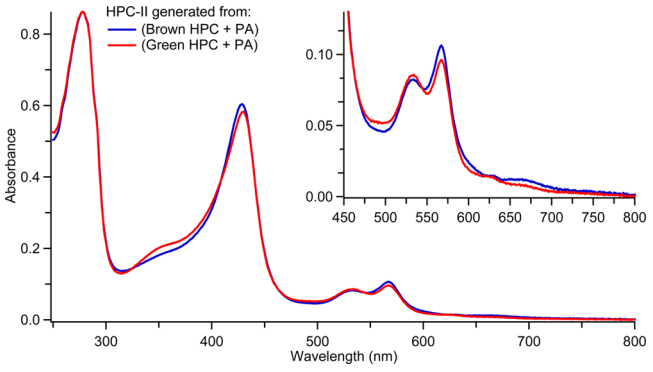

Figure 5. UV/visible spectral comparison of HPC-II formed from brown (blue) and green (red) ferric HPC. There are clear differences in the position of the Soret maximum and Q-band ratios.

Q-band intensities, with the α Q-band being more intense than the β band ($\alpha/\beta \approx 1.3$). The Mössbauer parameters of HPC-II prepared from both the brown and green ferric forms are identical (see below) and consistent with an Fe^{IV}–OH center, Figure 8.[28,29,32,34]

Although HPC-II can be obtained in high yield from either ferric form via the reaction with peracetic acid, the kinetics of the reactions are very different. In both cases, peracetic acid reacts with ferric enzyme to yield compound I, which then oxidizes the protein by one electron to generate compound II (similar behavior has been observed for cytochrome P450).[34] However, under conditions of low pH and high salt (green HPC), compound I formation is rate limiting. As a result, compound I does not accumulate, and the reaction with peracetic acid appears to generate compound II directly. In contrast, with low salt or high pH (brown HPC), the enzyme reacts with peracetic acid to generate compound I in almost 100% yield, which then decays in a slower process to compound II (see Supporting Information).

Using either ferric conformation, compound II could be prepared in >~90% yield. These high-purity compound II samples could then be mixed against strongly buffered, higher-pH solutions to interrogate HPC-II protonation from pH 9 to 14. While a majority of these experiments were initiated with the green ferric form, we also prepared HPC-II using the brown form at pH 5, 9, 13, and 13.6 to examine if similar results were obtained from either starting point. The above experiments allowed us determine the behavior of HPC-II as a function of pH.

X-ray Absorption Spectroscopy (XAS) of Catalase Intermediates. HPC-II (~90% yield, pH 5.3, green conditions), HPC-I (~80% yield, pH 7, brown conditions), and HPC (pH 5.3, green conditions) were prepared and characterized by EXAFS spectroscopy. Fe K-edge absorption edges show that both HPC-II and HPC-I lie ~2 eV higher in energy than the ferric enzyme (Figure 6). This is consistent

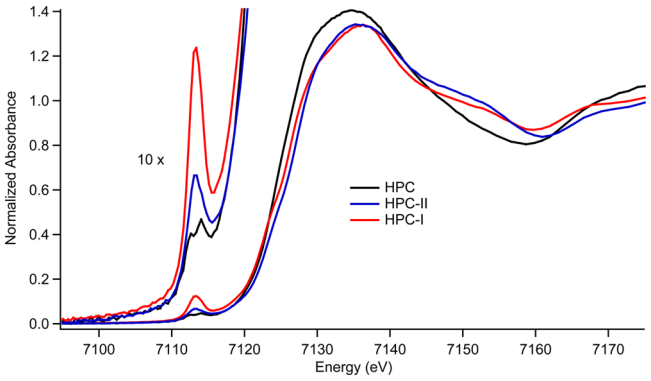

Figure 6. Fe K-edge X-ray absorption edges for HPC, HPC-I, and HPC-II.

with the assignment of both intermediates existing in a higher oxidation state (Fe^{IV}). There is also a large difference in the pre-edge intensity (1s→3d transition) between HPC-I and HPC-II. It is well known that a short metal–oxygen bond can create a highly asymmetric ligand environment, resulting in an intense pre-edge feature. As the metal–oxygen bond lengthens, the intensity of the pre-edge decreases.[41,53] This type of behavior suggests that HPC-I is unprotonated (Fe^{IV}=O), while HPC-II is better described as a protonated Fe^{IV}—OH intermediate.

Fits of the EXAFS data and Fourier transforms confirm the protonation assignments based on pre-edge trends, Figure 7. The Fe—O bond lengths are 1.66 and 1.78 Å for HPC-I (Fe^{IV}=O) and HPC-II (Fe^{IV}—OH), respectively, Table 1. These distances are in good agreement with DFT calculations and previously characterized compound I and compound II (protonated) heme intermediates.[28,30,34,36,54,55]

Mössbauer Spectroscopy. Mössbauer spectroscopy reveals small differences in the green and brown ferric forms of HPC, while the Mössbauer parameters obtained for HPC-II are independent of the color of the ferric enzyme used to prepare the intermediate. Figure 8 shows data obtained from the direct reaction of peracetic acid with both green and brown ferric forms at pH 5. HPC-II can be obtained in nearly quantitative yield in either case. Isomer shifts/quadrupole splittings for HPC-II prepared from green and brown enzyme are identical within experimental error (δ = 0.02 and ΔE_Q = 2.28 mm/s, and δ = 0.02 and ΔE_Q = 2.27 mm/s, respectively). These parameters, which are typical of an Fe^{IV}–OH species,[29,32,34] agree with the results obtained from our EXAFS measurements.

HPC-II can be prepared at higher pH via the direct reaction of brown HPC with peracetic acid. In one reaction that was mixed and frozen by hand at pH 9, we obtained roughly 15% HPC-II (Supporting Information). The remainder of the sample was HPC-I and ferric enzyme. The Mössbauer parameters of HPC-II obtained from this reaction are identical

DOI: 10.1021/jacs.6b09693
J. Am. Chem. Soc. 2016, 138, 16016–16023

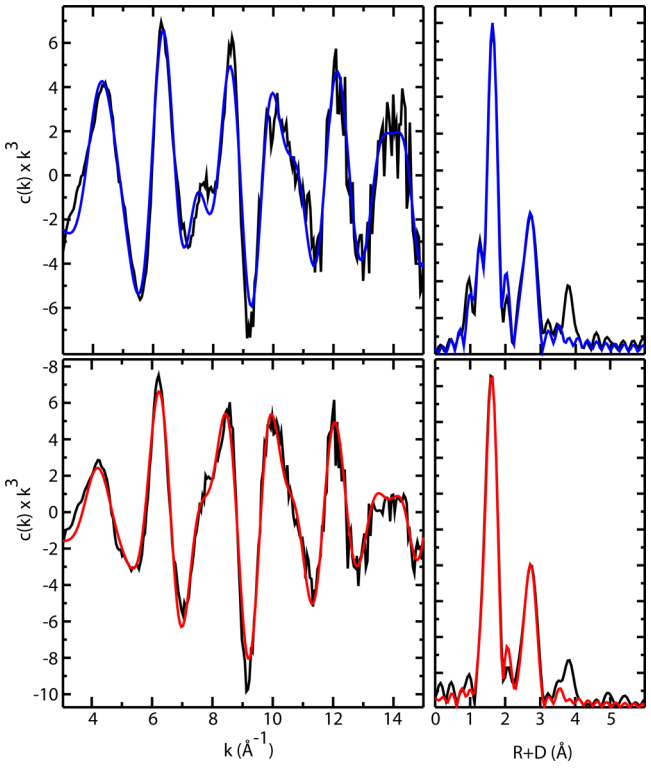

Figure 7. Fe K-edge EXAFS data (left) and Fourier transforms (right) of HPC-II (upper) and HPC-I (lower). Black lines show experimental data, and colored lines show the best fits. The fits shown were obtained over the region k = 3−15 Å^{-1}. All EXAFS samples were analyzed by Mössbauer spectroscopy prior to data collection.

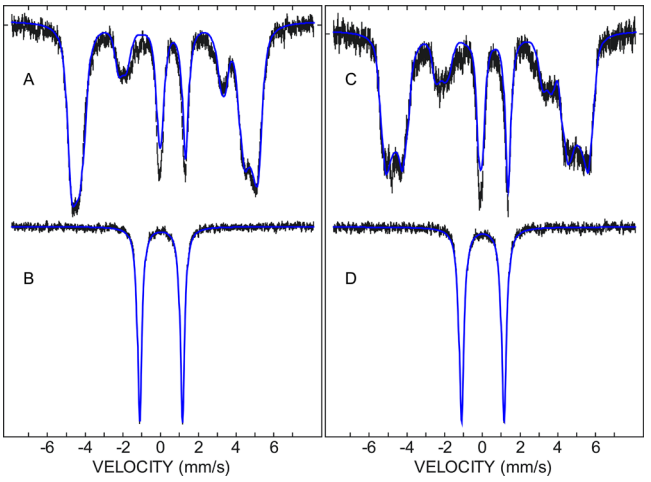

Figure 8. Mössbauer spectra of green/brown HPC and the products of their reactions with PA. Fits are in blue. (A) Green HPC (pH 5, 50 mM citrate, 500 mM NaCl) and (B) green HPC + PA (HPC-II). Isomer shift and quadrupole splitting values are δ = 0.02 and ΔE_Q = 2.28 mm/s. (C) Brown HPC (pH 5, 50 mM citrate, no salt) and (D) brown HPC + PA (HPC-II). Isomer shift and quadrupole splitting values are δ = 0.02 and ΔE_Q = 2.27 mm/s. HPC-II yield was >90%. Fit parameters for green/brown HPC are in Supporting Information.

to those at pH 5, indicating HPC-II is an iron(IV) hydroxide species at pH 9. There is no evidence of an iron(IV)-oxo species in the reaction mixture. Given the detection limit of the Mössbauer experiment (~3% total iron for the given sample), this result suggests a pK_a ≥ 10 for the iron(IV) hydroxide center of HPC-II.

In an effort to determine the pK_a of the HPC iron(IV) hydroxide species, we utilized the "pH-jump" method, similar to those employed to determine the pK_a of P450 compound II.[34] In these experiments HPC-II was made at pH 5 and quickly loaded into a syringe barrel at 4 °C. The syringe barrel was then placed in the freeze-quench apparatus, and HPC-II was mixed against strongly buffered, higher-pH solutions and subsequently sprayed into liquid ethane to stop the reaction. Using this technique, we observed only the hydroxide species up to pH 11. (Additional pH 11 experiments, in which mixing and freezing were performed by hand, yielded similar results.) Above pH 11, the hydroxide species begins to convert to a new species with Mössbauer parameters (σ = 0.08 mm/s, ΔE_Q = 1.51 mm/s) that are consistent with the formation of an Fe^{IV}=O intermediate, Figure 9.[23,28,34] A plot of the relative concentration of these species as a function of pH results in a titration curve with pK_a = 13.1, Figure 10. The pK_a of this transition appears to be independent of the ferric conformation (green or brown) used to prepare HPC-II at low pH (see Supporting Information).

We recently reported a pK_a ≈ 12 for the iron(IV) hydroxide state in P450-II in two different P450s, CYP158-II and CYP119-II.[34] In CYP158-II, the intermediate could be prepared

Table 1. EXAFS Fitting Results for HPC-II and HPC-I[a]

Fe−N			Fe−O*			Fe−O				
N	R	σ^2	N	R	σ^2	N	R	σ^2	E_0	error
					HPC-II					
5	**1.978**	**0.00206**	**0**			**1**	**1.775**	**0.00459**	**−13.397**	**0.3045**
5	1.992	0.00252	0			0			−8.9581	0.3326
4	1.980	0.00260	1	1.963	0.00117	1	1.776	0.00398	−13.196	0.3076
					HPC-I					
5	**2.004**	**0.00208**	**0**			**1**	**1.661**	**0.00234**	**−12.516**	**0.2325**
5	1.995	0.00203	0			0			−16.415	0.3473
4	1.999	0.00192	1	2.051	0.00124	1	1.662	0.00228	−12.403	0.2312

[a]Fe−O* corresponds to the oxygen from the proximal tyrosine residue. Raw data were fit over the region k = 3−15 Å^{-1}. Coordination number N, interatomic distance R (Å), mean square deviation in R (the Debye−Waller factor) σ^2 (Å^2), and the threshold energy shift E_0 (eV) are reported. The fit error is defined as $[\sum k^6(\chi_{exptl} - \chi_{calc})^2/\sum k^6 \chi^2_{exptl}]^{1/2}$. Best fits are shown in boldface. Alternative fits with and without the axial Fe−O* contribution are also shown. For the k-range examined, there is not enough resolution to distinguish between the heme nitrogens and the tyrosinate oxygen. Coordination numbers N were constrained during the fits.

DOI: 10.1021/jacs.6b09693
J. Am. Chem. Soc. 2016, 138, 16016−16023

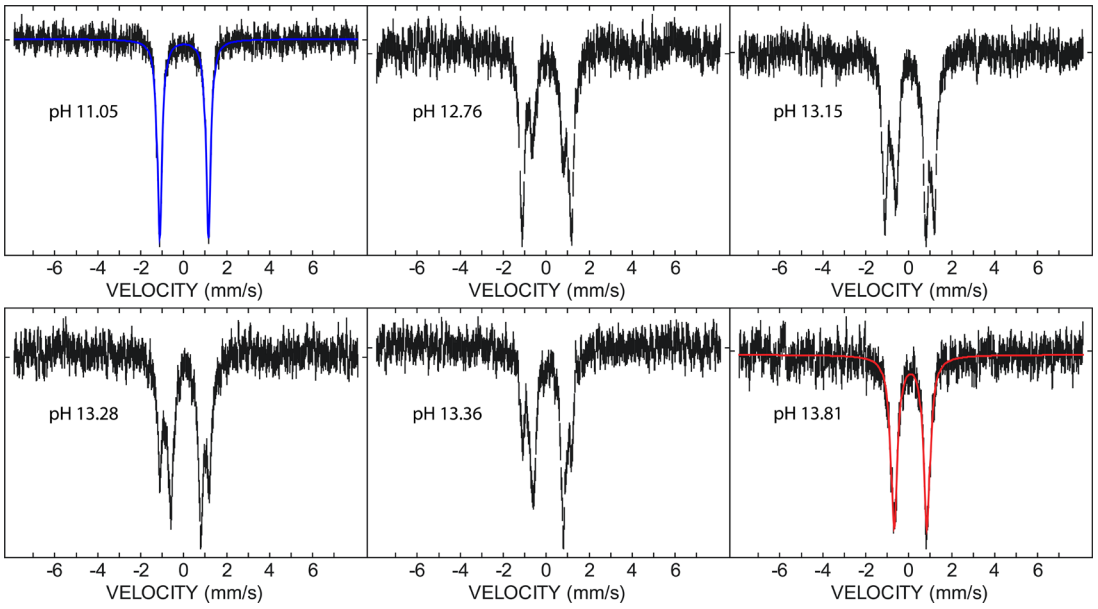

Figure 9. Mössbauer spectra of HPC-II at increasing pH. Approximately 65% high-pH ferric HPC was subtracted from all spectra except the pH 11.05 sample, which was generated in ~80% yield. Samples were prepared by a rapid freeze-quench experiment. A 4 mM HPC-II solution (pH 5.3) was prepared by adding 12.5 equiv of PA (in water) to green HPC at 4 °C. Upon compound II formation, the mixture was immediately loaded into a freeze-quench syringe and mixed 2:1 with an arginine/NaOH buffer (pH 14). The strength of the arginine/NaOH buffer was varied (54.08 mM – 216.32 mM) to achieve the desired pH. The reaction mixture was sprayed in liquid ethane ~2 ms after the pH-jump. The isomer shift/quadrupole splitting parameters are δ = 0.02 mm/s and ΔE_Q = 2.26 mm/s, and δ = 0.08 mm/s and ΔE_Q = 1.51 mm/s, for the HPC-II hydroxide (blue) and high-pH HPC-II (red) intermediates, respectively.

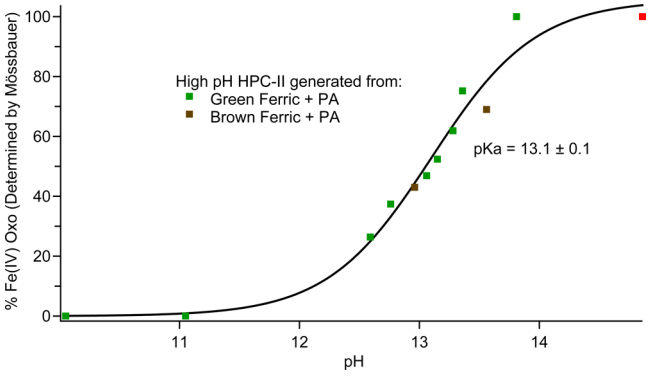

Figure 10. Mössbauer pH titration curve for HPC-II obtained by plotting the relative concentration of high-pH HPC-II (iron(IV)-oxo) as a function of increasing pH. The best-fit curve yields a pK_a of 13.1. Green data points are from samples prepared from green ferric + PA (HPC-II). Brown data points are from samples prepared from brown ferric + PA (HPC-II). The red data point is not from experiment but reflects the appropriate % of high-pH HPC-II (iron(IV)-oxo) at pH 14.81 (100%). It was added to improve the quality of the fit but does not change the experimentally determined pK_a (±0.1). A similar pK_a titration curve without the pH 14.81 data point is shown in Supporting Information (Figure S7). The equation used for fitting was $f(x) = (a + b \times 10^{(x-c)})/(1 + 10^{(x-c)})$.

in almost quantitative yield at high and low pH (13.3 and 9), and the transition could be followed using Mössbauer, UV/visible, and EXAFS spectroscopies. Additionally, CYP158-II was extraordinarily stable on the time scale of our rapid mixing experiments. This allowed for reversibility studies in which the intermediate was first deprotonated at high pH, and then reprotonated upon returning to neutral or slightly basic conditions. CYP119-II was not as well behaved at high pH, but insights gained from CYP158-II (principally the thiolate-ligated iron(IV)-oxo's UV/visible spectrum) helped to assign the transition in CYP119. All together, the full complement of these spectroscopic techniques is what permitted the definitive assignment of the iron(IV) hydroxide pK_a in both thiolate-ligated systems.

This was not the case with HPC-II. Because HPC-II degrades rapidly at pH > 12, low yields are extremely problematic. Furthermore, the UV/visible spectrum of a tyrosinate-ligated iron(IV)-oxo is unknown. These factors inhibited our ability to track the transition with UV/visible spectroscopy and to perform reversibility studies. The low yields also prohibited EXAFS characterization of the putative oxo species.

While there is a distinct possibility that this high-pH transition could correspond to the iron(IV) hydroxide pK_a for a tyrosine-ligated system, given the data, a definitive assignment cannot be made. Our data suggest that the pK_a of HPC-II is >11, but additional studies are needed to assign the transition at pH 13.1. There is also the potential likelihood that a different catalase enzyme could provide a more stable platform for this investigation. As noted, investigations of the pK_a of CYP119-II were complicated by partial degradation of the intermediate at high pH.[34] Only through the application of prior knowledge gained from CYP158-II were we able to assign the iron(IV) hydroxide pK_a in that system.

CONCLUSION

Using UV/visible, EXAFS, and Mössbauer spectroscopies, we have shown that HPC-II exists in an iron(IV) hydroxide state. The iron(IV) hydroxide state in P450 compound II is thought to be stabilized by strong electron donation from the anionic thiolate ligand.[30,34,56] The tyrosinate ligand in catalase is electron donating and has a similar charge. However, it was unclear if the highly conserved arginine (which forms non-covalent interactions with the tyrosinate) of catalase could

DOI: 10.1021/jacs.6b09693
J. Am. Chem. Soc. 2016, 138, 16016–16023

effectively negate the charge and/or reduce the electron-donating properties of the tyrosinate ligand enough to result in a more typical compound II species (i.e., an authentic iron(IV)-oxo complex). Our investigation suggests it does not.

We have argued that basic ferryl species can promote two-electron chemistry by suppressing off-pathway one-electron oxidations of the protein's superstructure.[34,35] The presence of a basic ferryl species in catalase is consistent with this suggestion. Two-electron chemistry is critical to catalase function: catalase must avoid the formation of compound II, which is a dead-end state for the enzyme. Previous investigations have shown that electron donors (e.g., phenols, alcohols, formate, and NADPH) can play a crucial role in preventing the buildup of the inactive compound II state.[1,46a,57,58] While these donors have typically been thought of as the primary safety valve for the recovery from off-pathway chemistry, our investigation suggests they are not the first line of defense. An elevated ferryl pK_a can decrease the one-electron reduction potential of compound I, diminish the driving force for compound II formation, and reduce the need for energetically expensive electron donor molecules.

MATERIALS AND METHODS

Growth and Purification of *Helicobacter pylori* Catalase (HPC). KatA, the gene encoding HPC, was cloned from a pSO100 plasmid (kindly provided by Prof. Peter Loewen) into a pET26b(+) vector and overexpressed in BL21 (DE3) (Novagen) competent cells. A starter culture was grown overnight (~16 h, 37 °C, 225 rpm) in LB media supplemented with 50 μg/mL of kanamycin. The starter was used to inoculate a larger (2−3 L of media) flask. At an OD of 0.8−1.0, 0.5 mM IPTG and δ-aminolevulinic acid were added along with an additional aliquot of kanamycin (25 μg/mL). The temperature and shaker speed were reduced to facilitate proper expression and folding of the protein (28 °C, 100 rpm).

After 24 h the cells were harvested, redissolved in buffer (50 mM Kphos, 50 mM EDTA, 1% Triton X-100 biological surfactant or 1% polyethylene glycol monododecyl ether, pH 7), and lysed using a microfluidizer processor (M-110EH-30). Protein was then initially purified by ammonium sulfate precipitation. Subsequent 40% and 50% fractions were discarded. Fractions between 50% and 80% were HPC containing. Pellets were resuspended in a minimum amount of 50 mM Kphos buffer (pH 7) and run down a DE-52 column (Whatman), separating a red band. Protein was then buffer exchanged into 50 mM citrate (pH 5) and loaded onto a Source S column (Whatman). HPC was washed with 2 column volumes of starting buffer and eluted using a 0−500 mM NaCl gradient of the same buffer. Fractions with R_z > 0.80 were pooled for use.

For ^{57}Fe enrichment, half of the total aliquot of ^{57}Fe was added at inoculation, and the other half was added at induction. Also added at induction were 0.5 mM δ-aminolevulinic acid and 1 mL/L of a solution of trace elements. The remaining steps are the same as in the rich media procedure.

Freeze-Quenched Samples. Freeze-quench methods were used to generate HPC-II at high pH. A four-syringe ram freeze-quench apparatus from Update Instruments (Madison, WI) was used for all freeze-quench experiments. Aqueous reaction mixtures were sprayed into liquid ethane (89 K). Liquid ethane was subsequently removed under vacuum in an isopentane bath (~120 K), and samples for Mössbauer and EXAFS were packed under liquid nitrogen.

Preparation of Ferric HPC, HPC-I, and HPC-II. *Ferric HPC.* Ferric HPC (4 mM, pH 5.3, 500 mM NaCl) was sprayed into liquid ethane (89 K). Liquid ethane was subsequently removed under vacuum in an isopentane bath (~120 K). Samples for Mössbauer and EXAFS were packed under liquid nitrogen.

HPC-I. Samples were prepared by mixing 3−5 mM ferric HPC (50 mM sodium phosphate, pH 7, no salt) with ~5 equiv of peracetic acid (PA, 32 wt% sol in dilute acetic acid, Sigma-Aldrich). Once the mixture turned from brown to green (1−2 s), the solution was pipetted into a falcon tube containing liquid ethane (89 K) to quench the reaction. Liquid ethane was subsequently removed under vacuum in an isopentane bath (~120 K). Samples for Mössbauer and EXAFS were packed under liquid nitrogen.

HPC-II Hydroxide. Samples were prepared by mixing 3−5 mM ferric HPC with 12.5 equiv of PA (in water). From pH 3.5 to 5.5 HPC was in citrate buffer (50 mM, with or without 500 mM NaCl) and from pH 5.5 to 8 HPC was in sodium phosphate buffer (50 mM, with or without 500 mM salt). Tris buffer (50 mM, with or without 500 mM NaCl) was used from pH 8 to 9. Once the mixture turned bright red, the solution was pipetted into a falcon tube containing liquid ethane (89 K) to quench the reaction. Liquid ethane was subsequently removed under vacuum in an isopentane bath (~120 K). Samples for Mössbauer and EXAFS were packed under liquid nitrogen.

HPC-II at High pH. First, 3−5 mM HPC-II was generated at pH 5.3 (50 mM citrate, 250 mM NaCl for green ferric or 50 mM citrate for brown ferric) prior to freeze-quenching by mixing with ~12.5 equiv of PA (in water, 4 °C). HPC-II was then rapidly loaded into the freeze-quench syringe (4 °C) and quenched 2:1 against an arginine HCl/sodium hydroxide buffer (pH 14). It is essential that the quench be executed within 1−2 min of initially making HPC-II because of the rapid decay of the intermediate. The strength of the buffer was varied (54.08−216.32 mM) to change the final pH of the solution, thus altering the ratio of compound II oxo/hydroxide. The reaction was quenched in a liquid ethane bath ~2 ms after mixing. Portions of the quenched samples were set aside to confirm the final pH of the solution. Samples were packed into Mössbauer sample cups for spectroscopic analysis at a final protein concentration of 3 mM.

Low-Concentration UV/Visible Experiments Performed in Cary UV/Vis. Using a molar extinction coefficient of $\varepsilon_{(406\ nm)} = 1.0 \times 10^5$ M^{-1} cm^{-1} for ferric catalase, generation of HPC-I/HPC-II was formed as follows. One mL of either green or brown ferric HPC was placed in a sample cuvette and approximately 50 μL of a PA solution (in water) containing 12.5 mol equiv was added. A glass pipet was used to mix the solution before the reaction was monitored over the course of several minutes.

Mössbauer Spectroscopy. A spectrometer from WEB Research (Edina, MN) was used to collect data in constant acceleration mode with a transmission geometry. Spectra were recorded with a 53 mT magnetic field applied parallel to the γ-beam. All measurements were recorded at 4.2 K using a Janis SVT400 cryostat. Isomer shifts were calibrated relative to the centroid of the spectrum of a metallic foil of α-Fe at room temperature. Data analysis was performed using the program WMOSS from WEB research.

X-ray Absorption Spectrsocopy (XAS). XAS data were collected in fluorescence mode at ~10 K with a 30-element germanium detector (SSRL, BL7-3) using a Si(220) Φ = 0° double monochromator with a 9.5 keV cutoff for harmonic rejection. To minimize the effects of photoreduction, samples were moved in the beam so that unexposed portions of the sample were examined every 2 scans (exposure time at ~37 min per scan). XAS were obtained by averaging 7 total scans (7 first scans) for ferric HPC, 18 total scans (9 first scans and 9 second scans) for HPC-I, and 21 total scans (15 first scans and 6 second scans) for HPC-II. The effects of photoreduction were monitored via the analysis of data obtained during the second acquisition scan. Background removal and curve fitting were performed with EXAFSPAK (available at http://www-ssrl.slac.stanford.edu/exafspak.html) using *ab initio* phases and amplitudes generated with FEFF version 8.0. Data sets were fit over the range k = 3−15 Å^{-1}. Coordination numbers N were constrained during the fits. Fits included first- and second-shell atoms and one multiple scattering component. In all cases, the second shell was comprised of α- and *meso*-carbons and the Fe−C_α−N−Fe multiple scattering paths (n = 8, 4, and 16, respectively). All distances R, and Debye−Waller factors σ^2, were treated as adjustable parameters, and all threshold energy shifts E_o were linked but allowed to vary. The passive electron reduction factor S_o was held at 0.9. Edge energies were calibrated using α-Fe metal foil (7111.3 eV). Edge positions were obtained from the first

DOI: 10.1021/jacs.6b09693
J. Am. Chem. Soc. 2016, 138, 16016−16023

derivative of the data using EXAFSPAK (1.0 eV smoothing, third-order polynomial).

■ ASSOCIATED CONTENT

Supporting Information

The Supporting Information is available free of charge on the ACS Publications website at DOI: 10.1021/jacs.6b09693.

Mössbauer and Mössbauer fit parameters, XAS edges, and UV/visible spectra (PDF)

■ AUTHOR INFORMATION

Corresponding Author

*m.green@uci.edu

Notes

The authors declare no competing financial interest.

■ ACKNOWLEDGMENTS

This work was supported by NIH (R01-GM101390). We thank M. Latimer and E. Nelson for onsite assistance at the synchrotron. Use of the Stanford Synchrotron Radiation Lightsource, SLAC National Accelerator Laboratory, is supported by the U.S. Department of Energy, Office of Science, Office of Basic Energy Sciences, under contract no. DE-AC02-76SF00515. The SSRL Structural Molecular Biology Program is supported by the DOE Office of Biological and Environmental Research and by the National Institutes of Health, National Institute of General Medical Sciences (including P41GM103393).

■ REFERENCES

(1) Dunford, H. B. *Peroxidases and Catalases: Biochemistry, Biophysics, Biotechnology, and Physiology*, 2nd ed.; John Wiley and Sons: New York, 2010.

(2) Makris, T. M.; von Koenig, K.; Schlichting, I.; Sligar, S. G. *J. Inorg. Biochem.* **2006**, *100*, 507.

(3) Sono, M.; Roach, M. P.; Coulter, E. D.; Dawson, J. H. *Chem. Rev.* **1996**, *96*, 2841.

(4) Denisov, I. G.; Makris, T. M.; Sligar, S. G.; Schlichting, I. *Chem. Rev.* **2005**, *105*, 2253.

(5) Ortiz de Montellano, P. R. *Cytochrome P450: Structure, Mechanism, and Biochemistry*, 3rd ed.; Kluwer Academic/Plenum Publishers: New York, 2004; Vol. ed. 3.

(6) Krebs, C.; Fujimori, D. G.; Walsh, C. T.; Bollinger, J. M. *Acc. Chem. Res.* **2007**, *40*, 484.

(7) Wong, S. D.; Srnec, M.; Matthews, M. L.; Liu, L. V.; Kwak, Y.; Park, K.; Bell, C. B., III; Alp, E. E.; Zhao, J. Y.; Yoda, Y.; Kitao, S.; Seto, M.; Krebs, C.; Bollinger, J. M.; Solomon, E. I. *Nature* **2013**, *499*, 320.

(8) Han, S. W.; Ching, Y. C.; Rousseau, D. L. *Nature* **1990**, *348*, 89.

(9) Wikstrom, M. *Nature* **1989**, *338*, 776.

(10) Chance, B. *Arch. Biochem.* **1949**, *21*, 416.

(11) Paeng, K. J.; Kincaid, J. R. *J. Am. Chem. Soc.* **1988**, *110*, 7913.

(12) Sitter, A. J. *J. Biol. Chem.* **1985**, *260*, 7515.

(13) Pennerhahn, J. E.; Eble, K. S.; McMurry, T. J.; Renner, M.; Balch, A. L.; Groves, J. T.; Dawson, J. H.; Hodgson, K. O. *J. Am. Chem. Soc.* **1986**, *108*, 7819.

(14) Rutter, R.; Valentine, M.; Hendrich, M. P.; Hager, L. P.; Debrunner, P. G. *Biochemistry* **1983**, *22*, 4769.

(15) Lamar, G. N.; Deropp, J. S.; Smith, K. M.; Langry, K. C. *J. Biol. Chem.* **1981**, *256*, 237.

(16) Roberts, J. E.; Hoffman, B. M.; Rutter, R.; Hager, L. P. *J. Biol. Chem.* **1981**, *256*, 2118.

(17) Roberts, J. E.; Hoffman, B. M.; Rutter, R.; Hager, L. P. *J. Am. Chem. Soc.* **1981**, *103*, 7654.

(18) Chin, D. H.; Balch, A. L.; Lamar, G. N. *J. Am. Chem. Soc.* **1980**, *102*, 1446.

(19) Chin, D. H.; Lamar, G. N.; Balch, A. L. *J. Am. Chem. Soc.* **1980**, *102*, 5945.

(20) Groves, J. T.; Haushalter, R. C.; Nakamura, M.; Nemo, T. E.; Evans, B. J. *J. Am. Chem. Soc.* **1981**, *103*, 2884.

(21) Pennerhahn, J. E.; McMurry, T. J.; Renner, M.; Latosgrazynsky, L.; Eble, K. S.; Davis, I. M.; Balch, A. L.; Groves, J. T.; Dawson, J. H.; Hodgson, K. O. *J. Biol. Chem.* **1983**, *258*, 2761.

(22) Deropp, J. S.; Lamar, G. N.; Wariishi, H.; Gold, M. H. *J. Biol. Chem.* **1991**, *266*, 15001.

(23) Simonneaux, G.; Scholz, W. F.; Reed, C. A.; Lang, G. *Biochim. Biophys. Acta, Gen. Subj.* **1982**, *716*, 1.

(24) Rittle, J.; Green, M. T. *Science* **2010**, *330*, 933.

(25) Bell, S. R.; Groves, J. T. *J. Am. Chem. Soc.* **2009**, *131*, 9640.

(26) Wang, X. S.; Peter, S.; Kinne, M.; Hofrichter, M.; Groves, J. T. *J. Am. Chem. Soc.* **2012**, *134*, 12897.

(27) Yosca, T. H.; Green, M. T. *Isr. J. Chem.* **2016**, *56*, 834.

(28) Behan, R. K.; Green, M. T. *J. Inorg. Biochem.* **2006**, *100*, 448.

(29) Behan, R. K.; Hoffart, L. M.; Stone, K. L.; Krebs, C.; Green, M. T. *J. Am. Chem. Soc.* **2006**, *128*, 11471.

(30) Green, M. T.; Dawson, J. H.; Gray, H. B. *Science* **2004**, *304*, 1653.

(31) Stone, K. L.; Behan, R. K.; Green, M. T. *Proc. Natl. Acad. Sci. U. S. A.* **2006**, *103*, 12307.

(32) Stone, K. L.; Hoffart, L. M.; Behan, R. K.; Krebs, C.; Green, M. T. *J. Am. Chem. Soc.* **2006**, *128*, 6147.

(33) Wang, X. S.; Ullrich, R.; Hofrichter, M.; Groves, J. T. *Proc. Natl. Acad. Sci. U. S. A.* **2015**, *112*, 3686.

(34) Yosca, T. H.; Rittle, J.; Krest, C. M.; Onderko, E. L.; Silakov, A.; Calixto, J. C.; Behan, R. K.; Green, M. T. *Science* **2013**, *342*, 825.

(35) Yosca, T. H.; Behan, R. K.; Krest, C. M.; Onderko, E. L.; Langston, M. C.; Green, M. T. *J. Am. Chem. Soc.* **2014**, *136*, 9124.

(36) Green, M. T. *J. Am. Chem. Soc.* **2006**, *128*, 1902.

(37) Chance, M.; Powers, L.; Kumar, C.; Chance, B. *Biochemistry* **1986**, *25*, 1259.

(38) Chance, M.; Powers, L.; Poulos, T.; Chance, B. *Biochemistry* **1986**, *25*, 1266.

(39) Hashimoto, S. *J. Biol. Chem.* **1986**, *261*, 11110.

(40) Hashimoto, S.; Tatsuno, Y.; Kitagawa, T. *Proc. Natl. Acad. Sci. U. S. A.* **1986**, *83*, 2417.

(41) Penner-Hahn, J. E.; Hodgson, K. O. *Iron Porphyrins*; VCH: New York, 1989; Vol. *III*.

(42) Sitter, A. J.; Reczek, C. M.; Terner, J. *Biochim. Biophys. Acta, Protein Struct. Mol. Enzymol.* **1985**, *828*, 229.

(43) Terner, J.; Palaniappan, V.; Gold, A.; Weiss, R.; Fitzgerald, M. M.; Sullivan, A. M.; Hosten, C. M. *J. Inorg. Biochem.* **2006**, *100*, 480.

(44) Meharenna, Y. T.; Doukov, T.; Li, H. Y.; Soltis, S. M.; Poulos, T. L. *Biochemistry* **2010**, *49*, 2984.

(45) Ma, Z. X.; Williamson, H. R.; Davidson, V. L. *Proc. Natl. Acad. Sci. U. S. A.* **2015**, *112*, 10896.

(46) (a) Loewen, P. C.; Carpena, X.; Rovira, C.; Ivancich, A.; Perez-Luque, R.; Haas, R.; Odenbreit, S.; Nicholls, P.; Fita, I. *Biochemistry* **2004**, *43*, 3089. (b) Alfonso-Prieto, M.; Borovik, A.; Carpena, X.; Murshudov, G.; Melik-Adamyan, W.; Fita, I.; Rovira, C.; Loewen, P. C. *J. Am. Chem. Soc.* **2007**, *129*, 4193. (c) Alfonso-Prieto, M.; Oberhofer, H.; Klein, M. L.; Rovira, C.; Blumberger, J. *J. Am. Chem. Soc.* **2011**, *133*, 4285.

(47) (a) Murshudov, G. N.; Grebenko, A. I.; Brannigan, J. A.; Antson, A. A.; Barynin, V. V.; Dodson, G. G.; Dauter, Z.; Wilson, K. S.; Melik-Adamyan, W. R. *Acta Crystallogr., Sect. D: Biol. Crystallogr.* **2002**, *58*, 1972. (b) Rovira, C. *ChemPhysChem* **2005**, *6*, 1820.

(48) Chuang, W. J.; Heldt, J.; Vanwart, H. E. *J. Biol. Chem.* **1989**, *264*, 14209.

(49) Horner, O.; Mouesca, J. M.; Solari, P. L.; Orio, M.; Oddou, J. L.; Bonville, P.; Jouve, H. M. *JBIC, J. Biol. Inorg. Chem.* **2007**, *12*, 509.

(50) Horner, O.; Oddou, J. L.; Mouesca, J. M.; Jouve, H. M. *J. Inorg. Biochem.* **2006**, *100*, 477.

(51) Harami, T. *J. Chem. Phys.* **1979**, *71*, 1309.

(52) Parak, F.; Bade, D.; Marie, A. L. *J. Phys. Colloques* **1979**, *40*, C2-528.

DOI: 10.1021/jacs.6b09693
J. Am. Chem. Soc. 2016, 138, 16016−16023

(53) Rohde, J. U.; Torelli, S.; Shan, X. P.; Lim, M. H.; Klinker, E. J.; Kaizer, J.; Chen, K.; Nam, W. W.; Que, L. *J. Am. Chem. Soc.* **2004**, *126*, 16750.
(54) Krest, C. M.; Silakov, A.; Rittle, J.; Yosca, T. H.; Onderko, E. L.; Calixto, J. C.; Green, M. T. *Nat. Chem.* **2015**, *7*, 696.
(55) Stone, K. L.; Behan, R. K.; Green, M. T. *Proc. Natl. Acad. Sci. U. S. A.* **2005**, *102*, 16563.
(56) Sono, M.; Andersson, L. A.; Dawson, J. H. *J. Biol. Chem.* **1982**, *257*, 8308.
(57) Kirkman, H. N.; Rolfo, M.; Ferraris, A. M.; Gaetani, G. F. *J. Biol. Chem.* **1999**, *274*, 13908.
(58) Hillar, A.; Nicholls, P.; Switala, J.; Loewen, P. C. *Biochem. J.* **1994**, *300*, 531.

DOI: 10.1021/jacs.6b09693
J. Am. Chem. Soc. 2016, 138, 16016−16023